RSC Advances

ROYAL SOCIETY
OF CHEMISTRY

www.rsc.org/advances

1

2

One-step synthesis of cellulose/silver nanobiocomposites using solution plasma process

and characterization of their broad spectrum antimicrobial efficacy

5

[a]MubarakAli Davoodbasha, [b]Sang-Yul Lee, [b]Seoung-Cheol Kim, and [a, *]Jung-Wan Kim

[a]*Division of Bioengineering, College of Life Science and Bioengineering, Incheon National University, Republic of Korea.*

[b]*Center for Surface Technology and Applications, Department of Materials Engineering, Korea Aerospace University, Republic of Korea.*

11

12

13

*Corresponding author

Jung-Wan, Kim. Ph.D

Professor

Division of Bioengineering

Incheon National University

Republic of Korea

Phone: +82-32-835-8244

Fax: +82-32-835-0804

E.Mail: kjw5854@incheon.ac.kr

23

1

Abstract

3   Solution plasma process (SPP) is a one-step synthesis technique which expeditiously produces

4   ultra-pure, stable, and uniform nanoparticles in polymer solution with plasma discharge.   Silver

5   nanoparticles (AgNPs) were synthesized in a cellulose matrix as biocomposites by discharging

6   plasma for 180 s at 800 V with a frequency of 30 kHz using a pulsed unipolar power supply into

7   solutions containing cellulose (1-3%) and $AgNO_3$ (1-5mM).   3D scaffolds of the resulting

8   cellulose/AgNP biocomposites were prepared by lyophilization and cross-linked with UV

9   irradiation.   UV-Vis spectroscopy showed a characteristic absorbance maximum in the range of

10   350-440 nm for the AgNP biocomposites with increase in the intensity of the peaks as the

11   concentration of $AgNO_3$ increased.   The peaks exhibited transition to red shift due to AgNP

12   formation.   The nanobiocomposites were pure when examined by FTIR spectrum.   3D scaffolds

13   had micro-porous structure with pores of (68-74) ± 2 μm in diameter when observed using FE-

14   SEM equipped with EDS.   TEM analysis showed that spherical AgNPs in the size range of 5-30

15   nm were well distributed in the biocomposites of C3Ag3 and C3Ag5.   The nanobiocomposites

16   had a broad spectrum of antimicrobial activity against various pathogens with a minimal inhibition

17   concentration of 5.1-20.4 μg/ml for bacteria and 81.6-255.0 μg/ml for fungi.   They killed gram

18   negative bacteria most effectively, but did not affect fungal growth very well, implying their

19   potential as topical antimicrobial agents for topical treatment of wounds.   SPP seemed to be the

20   most effective and safest method to synthesize various biocompatible polymer-metal nanoparticle

21   biocomposites.

22

1

3

1   **Introduction**

2   The perpetual copious research, which continues to provide new illuminating scientific data,

3   validates the desideratum for continuation in the research, development, and analysis of the

4   synthesis of nanomaterials by physical, chemical and biological routes for its application as

5   nanotechnology in general and nanomedicine in particular.   Generation of nanoparticles,

6   typically by either chemical or physical methods often requires addition of toxic chemicals,

7   expensive equipment, and mostly multiple steps[1].   During the biological route, two consecutive

8   steps of synthesis and purification of nanoparticles resulted in the production of nanoparticles

9   having biomolecules on the surface, which could then trigger egregious signals during utilization[2].

10   Insufficient synthesis methodologies to prevent incorporation of additives, detergents, or

11   chemicals that might not completely be removed can also contribute to toxicity of nanoparticles

12   prepared[3].

13   Solution plasma process (SPP) is an ideal method for the synthesis of nanoparticles without

14   adding toxic chemical reagent and with no need of expensive instrument.   However, SPP has not

15   been employed widely for the purpose, despite the extensive scientific evidence and its

16   potentiality in application to materials science and medicine[4,5]. SPP involves a sequence of

17   physical and chemical reactions, in which the water molecules splits into free radicals (H$^{\cdot}$, OH$^{\cdot}$,

18   electrons, UV) and solutes (precursors) into ions to nanoparticles during the discharge of plasma

19   in the solution[6].   Faster chemical reactions at lower temperature with greater variability are

20   possible by plasma generated in solution of various solutes and solvents, since density of

21   molecules in the liquid phase is much higher than that of the gas phase[7].   SPP can be widely used

22   for degradation of polymers, surface coating, and fabrication of materials at the nanoscale level

23   with various dimensions and structure[8-10].   Especially, nanoparticles synthesized can be

24   simultaneously fabricated into macromolecular polymers by SPP such that the particles are evenly

25   scattered in the matrix without agglomeration by forming 3D scaffold.   Thereby, plasma plays an

1   active role in the synthesis and stabilization of nanoparticles derived from the solutes in the

2   solution without adding hazardous chemicals[11-13].

3   The meticulous evidence-based researches, analyses, and reviews on plasma mediated synthesis

4   of nanomaterials, identifies the growing prospective of validating it's applicability in material

5   science, biomedicine, and particularly in nanomedicine[4].   Generation of nanomaterials (metals,

6   oxides, composites, polymers) using plasma in liquids by adding hazardous chemicals for

7   reduction and stabilization was reviewed extensively and summarized regarding their sizes and

8   applications in Table 1**.**   There was strong evidence that the interaction between nanoparticles

9   and polymers was responsible for the alteration in electrical and thermo-mechanical properties,

10   increasing specific surface area with decreasing particle size, and that the amount of interfacial

11   polymer layer strongly depends on size and concentration[26].

12   Among diverse nanomaterials, significant focus has been made on silver (Ag) due to its unique

13   properties, such as conductivity, stability, catalytic, and antimicrobial properties[2].   Silver and

14   silver based composites have been reported to exhibit antimicrobial activity against a wide range

15   of microorganisms such as bacteria, fungi, protozoa, and recently virus[26]**.**   It is of paramount

16   significance to develop, identify, validate, and employ an enhanced synthesis of polymer-metal

17   composites that are effective against pathogens, since various multidrug resistant pathogens which

18   are not controlled by commercial antibiotics, have been emerged and threatening human society

19   seriously[27].   Silver nanoparticles (AgNPs) well distributed in non-toxic and stable biological

20   polymers such as cellulose, one of the most abundant biomass on earth, would maximize its

21   potential as an antimicrobial agent against pathogens without causing their resistance to it.

22   Therefore, in this study, synthesis of cellulose/AgNP biocomposites was attempted using one-

23   step SPP without addition of any hazardous chemicals as reducing and/or stabilizing agents.

24   Physical and chemical parameters were optimized for the synthesis of the biocomposites and the

25   resulting biocomposites were characterized by adopting TEM, FE-SEM, EDS, FTIR, and UV-Vis

1   spectroscopy.   Additionally, cellulose/AgNP biocomposites were assessed for their antimicrobial

2   activity against several human pathogens such as bacteria (*Escherichia coli, Pseudomonas*

3   *aeruginosa, Vibrio parahaemolyticus, Staphylococcus aureus* and *Bacillus cereus*), yeast

4   (*Candida albicans*), and mold (*Aspergillus parasiticus*).   To our knowledge, this may be the first

5   work on the generation of cellulose/AgNP biocomposites by SPP for medicinal application, which

6   might be applied to topical wound healing materials significantly reducing microbial infection and

7   promoting recovery of dermal disease.

8

9   **2. Materials and methods**

10   **2.1. Solution plasma process set up**

11   Briefly, 150 ml of solution containing 1, 3, or 5 mM silver nitrate ($AgNO_3$, Junsei Co., Japan)

12   and 1, 2, or 3% hydroxylprophyl methylcellulose (HPMC, AN4, Samsung Fine Chemicals, Ltd.,

13   Korea) was mixed in a 200 ml pyrex beaker specially designed for the process in ambient

14   condition as described previously[28].   Plasma was generated using a pulsed field unipolar power

15   supply (IAP-1010, EN Technology, Korea) in the solution with a voltage, frequency, pulse width,

16   electrode distance, and discharge time of 800 V, 30 kHz, 2 μs, 1 mm, and 3 min, respectively.

17   A magnetic stirrer was used for the constant mixing and complete dispersion of the solutes in the

18   solution.   In order to understand the consequence of plasma discharged in the solution, pH,

19   temperature, and color change were observed and recorded periodically at every 1 min throughout

20   the experimental process.   The product of the process were notated as CxAgy, where x and y

21   represents the concentration of cellulose and silver nitrate, respectively.

22

23   **2.2. Fabrication of cellulose/AgNP**

24   Cellulose/AgNP biocomposites were successfully fabricated using the freeze drying

1   (lyophilization) method.   Briefly, 5 ml of synthesized nanoparticle biocomposites was transferred

2   into a sterile petri dish and frozen at -80°C overnight in a deep freezer (Forma Scientific, USA).

3   The frozen samples were lyophilized at -40°C with the pressure of 6.38 x 10^{-4} MPa using a freeze

4   dryer (FDV-7024, OPERON, Korea).   The dried samples were cross linked by UV irradiation

5   (254 nm) for 30 min to reduce water solubility.

6

7   **2.3. Characterization of cellulose/AgNP biocomposites**

8   Generation of AgNPs in the cellulose matrix using solution plasma was initially confirmed by

9   an UV-Visible spectrophotometer (UV -3600, UV Vis NIR spectrophotometer, Schimadzu, Japan)

10   in the range of 200 nm -1200 nm.   Viscosity of the synthesized biocomposites was also assessed

11   using a viscometer (Vibro SV-100, A&D Co., Japan) at room temperature.   An apparent

12   distribution of AgNPs was observed using a transmission electron microscope (TEM; JEOL-JSM,

13   JOEL Ltd., Japan).   Structure, texture, and porosity of 3D scaffold were examined by a field

14   emission scanning electron microscope (FESEM; JEOL-JSM-7001F, JEOL Ltd., Japan) equipped

15   with an energy dispersive spectroscopy in order to assess the elemental percentage within the

16   biocomposite.   Both purity and functional association of the biocomposite were studied using a

17   fourier transform infrared spectroscopy (FTIR; Vertex 8V, Bruker, Germany) in the ranges of 400

18   cm^{-1} to 4,000 cm^{-1}.

19

20   **2.4. Cultivation of microorganisms**

21   Seven microbial pathogens including *E. coli, P. aeruginosa, V. parahaemolyticus, S. aureus,*

22   and *B. cereus* (bacteria), *A. parasiticus* (fungus), and *C. albicans* (yeast) were used to test

23   antimicrobial activity of cellulose/AgNP biocomposites.   Bacteria were cultured in Luria-Bertani

24   medium (LB; yeast extract 0.5%, NaCl 0.5%, tryptone 1%) at 37°C; *A. parasiticus* in potato

1   dextrose medium (PD; potato dextrose 2.4%) at 25°C; and *C. albicans* in yeast peptone medium

2   (YPD; yeast extract 1%, peptone 2%, dextrose 2%) at 30°C.   Agar (1.5%) was added to each

3   medium when it was used as solid plates.   The amount of the cells was determined using the

4   McFarland standard.

5

6   **2.5. Evaluation of antimicrobial properties of cellulose/AgNP biocomposites**

7   *2.5.1. Agar Diffusion assay*

8   Antimicrobial property of the biocomposite scaffold was assessed by inhibiting microbial

9   reproduction on agar plate, which resulted in the formation of a clear zone around the disc

10   according to the Kirby-Bauer agar diffusion method[29].   About 10^{4} colony forming units (CFUs)

11   of freshly cultured microbial cells or fungal spores were spread on Műller-Hinton agar plates

12   (beef extract 0.2%, acid digest of casein 1.75%, starch 0.15%, Agar 1.7%; Difco Co., USA) and

13   discs of the C3/Ag1, Ag3, or Ag5 biocomposite scaffolds (6 mm in diameter) were placed on

14   them aseptically.   The resulting zone of growth inhibition was measured to assess antimicrobial

15   effect in 24 h (bacteria), 48 h (yeast), or 72 h (fungus) of incubation at an appropriate temperature

16   as described above.

17

18   *2.5.2. Minimal inhibitory concentration (MIC) of cellulose/AgNPs*

19   MIC of the biocomposites for each microorganism was determined by adding 0.0–326 μg/ml of

20   AgNP using the biocomposite of C3Ag5 to each microbial liquid culture (1-2 x 10^{5} CFU; 5 ml).

21   The tubes were incubated at 37°C for 18–24 h with gentle shaking.   MIC was determined as the

22   lowest concentration of the nanobiocomposites that produced no visible microbial growth (no

23   turbidity) in comparison with that of the control tube to which no nanobiocomposites was added.

24

25   *2.5.3. Reduction of CFU assay*

1   Bactericidal effect of cellulose/AgNP biocomposites was assessed quantitatively by monitoring

2   reduction of CFU upon treatment with nanobiocomposites during incubation. The amount of

3   cellulose/AgNP biocomposites to add was determined based on the MIC results. A precise

4   amount of each cellulose/AgNP biocomposite was added to LB broth inoculated with either *E.coli*

5   or *S.aureus* ($\sim 10^6$ CFU/ml) and incubated at 37^oC for 1-16 h. Cellulose free of AgNP was used

6   as control in all of the experimental sections. During incubation, an aliquot of culture was taken

7   periodically and inoculated on LB agar plates after appropriate dilution to determine CFU

8   remained by incubating at 37^oC overnight.

9

10   **2.5.4. Inhibition assay of fungal growth**

11   Effect of the nanobiocomposites on mycelia growth of *A. parasiticus* was examined by placing

12   a block of fungal hyphae (6 mm) on the centre of a PDA plate that had been smeared with 200 μl

13   of cellulose/AgNP biocomposites. A PDA plate with no nanobiocomposites smeared was used

14   as control. All of the plates were incubated for 72-120 h at 25^oC before observation on

15   morphology, hyphal growth, and sporulation pattern via pigmentation of sporangium.

16

17   **3. Results and Discussion**

18   **3.1. Synthesis of cellulose/AgNP biocomposites**

19   Analysis of the credible scientific data produced in this current study proved that pure, stable,

20   and hazardous chemical free cellulose/AgNs biocomposites were successfully synthesized by the

21   one-pot synthesis method of SPP. A total of 9 different biocomposites was prepared with

22   various combinations of cellulose (1, 2, 3%) and AgNO$_3$ (1, 3, 5 mM) concentrations. The initial

23   pH, temperature, and color of the solution was noted as 7.0±0.2, 28^oC, and a pale white color,

24   respectively, before plasma discharge. Once plasma was discharged, the solutions turned to

1 brown. This could be due to the reduction of silver from ionic (Ag^+) into metallic (Ag^0)

2 nanoparticles in the cellulose matrix by the active species of free radicals generated by solution

3 plasma. The intensity of color developed was reported to be dependent on the concentration of

4 $AgNO_3$ and polymer in use as well as the discharge time[16]. Previously, similar color change was

5 observed during synthesis of AgNPs using gelatin as the polymer matrix[26]. During the process,

6 pH of the solution was slightly decreased into acidic pH (6.0 ± 0.2) and temperature was raised

7 upto 90^oC. The viscosity of the solutions increased due to varying concentrations of cellulose

8 used such that 1%, 2% and 3% of cellulose solution had viscosity of 3.0, 7.6 and 7.8 cps,

9 respectively after plasma discharge for 180 s. It is of paramount significance that quality,

10 assurance, and efficacy of nanobiocomposites synthesized for biomedical applications need to be

11 meticulously monitored, reviewed, and improved to ensure all healthcare providers and patients

12 have accessibility to most effective applications for treatment. Currently a significant portion of

13 synthesized nanobiocomposites used in biomedical application, require a series of reactions which

14 use hazardous chemicals as reducing and stabilizing agents that may cause toxicity to normal cells.

15 SPP, an eco-friendly process, which synthesizes pure and, stable nanobiocomposites without

16 employing reducing and stabilizing agent, may provide an ideal method for producing superior

17 medical grade nanobiocomposites.

18 Formation of AgNPs in the solution was confirmed further by spectrophotometry and FTIR

19 spectroscopy. UV-Vis spectra were acquired for 9 cellulose/AgNP biocomposites of various

20 concentrations of cellulose and $AgNO_3$. Among them, the spectra of the nanobiocomposites

21 based on 3% cellulose displayed the most significant surface plasmon resonance (SPR) band (Fig.

22 1). An absorbance maximum was obtained in the range of 350-440 nm, a characteristics peak of

23 AgNPs due to SPR in the solution. A characteristic SPR band for AgNPs of C3Ag1, C3Ag3,

24 and C3Ag5 was centered at 358 nm, 438 nm, and 440 nm, respectively, increasing the intensity of

25 the SPR peaks as the concentration of the precursor ($AgNO_3$) increased. The peaks exhibited

10

1   transition to red shift due to AgNPs formed at various shapes, sizes, and the concentration of

2   silver used.   It has been reported that blue shift of a peak could be generated by the formation of

3   smaller particles when high concentrations of polymer were used[28].   In the previous report,

4   formation of AgNPs in the gelatin matrix was confirmed by the spectrophotometry, showing red

5   shift of SPR when more silver was used and the blue shift when more gelatin was used as the

6   matrix[26].

7   Purity of the nanobiocomposites of C3Ag1, C3Ag3, and C3Ag5 was examined by FTIR

8   spectroscopy (Fig. 2).   The characteristic peaks of cellulose such as O-H stretching, C-H

9   stretching, C-H wagging, C-H bending, and C-O stretching were observed[30].   The spectra of the

10   biocomposites of cellulose/AgNPs showed broadening, presence, and absence of peaks probably

11   due to the cellulose molecules interacting with silver ions[31].   The vibration at 1409.6 cm^{-1} and

12   1053.3 cm^{-1} was likely to represent C-H bending and C-OH bending, respectively, which might

13   play a functional role for the capping of AgNPs in the cellulose matrix. Additionally, vibrations at

14   1383 cm^{-1} and 728 cm^{-1} was corresponds to the C-H and $-CH_3$ groups present in the HPMC.

15   These functional groups confer surplus stability to the matrix.

16

17   **3.2. Physical properties of cellulose/AgNP biocomposites**

18   Microporous 3D scaffolds of the cellulose/AgNP biocomposites synthesized using various

19   concentrations of cellulose and $AgNO_3$ were prepared by lyophilization and they were cross-

20   linked with UV irradiation to increase water insolubility (Fig 3A, B).   Through this process, the

21   nanobiocomposites could also be sterilized.   The scaffolds made of low percentage of cellulose

22   (1% or 2%) showed unstable and fragile texture, whereas that of 3% cellulose was quite stable and

23   firm.   Moreover, it has been suggested that high viscosity of biocomposite was suitable for

24   scaffold formation[26].

25   The 3D scaffolds with microporous structures of the cellulose/AgNP biocomposites were

1   observed using FESEM equipped with EDS.   Microstructures of the biocomposites, C3Ag1,

2   C3Ag3, and C3Ag5 were slightly different from each other's, having inter-linked and multi-

3   walled structures (Fig. 3).   Significant fibril like structures were formed on the edges of C3Ag3

4   and C3Ag5, so called micro-fibrils.   The micro-fibril structures are important features of the

5   cellulose polymer; it could be useful for the scaffold for cell proliferation in tissue engineering

6   application[32].   Grande *et al.* reported that cellulose based nanocomposites showed good

7   biocompatibility and had high potential for the development of artificial skin and other type of

8   tissues[33].   For the purpose, the pore size, pore orientation, fibre structure and fibre diameter of

9   3D scaffolds were the important factors.

10   The mean diameter of the pores of C3Ag3 and C3Ag5 was calculated to be 68 ± 2 and $7\ 4\pm 2$

11   μm, respectively (Fig 3D, E).   The pore size was dependent on the amount of cellulose, which

12   affected the viscosity of the biocomposites[26].   The cellulose biocomposites synthesized in this

13   study had much higher viscosity (3.0-7.8 cps) and larger pore size than gelatin biocomposites

14   (2.4-4.8 cps; 17.67 ± 7.2 - 26.52 ± 12.8 μm).   When gelatin biocomposites were synthesized by

15   longer plasma discharge (780 s), they showed lower viscosity and smaller pore size than those

16   synthesized by shorter discharge (180 s).   This could be due to degradation of the gelatin

17   molecules into smaller molecules, which then resulted in deformation of connected micro pores[26,

18   34].   The topographic evaluation identified the location of spherical shaped AgNPs that were

19   encrusted on the cellulose matrix ranging from 15-20 nm in size (Fig. 3F).

20   EDS analysis showed that elements of C, O, and Ag in the constitution of the C3Ag5

21   biocomposites and percentage of the elements varied according to the concentrations of cellulose

22   and silver (Fig. 4).   The Ag element in the C3Ag5 biocomposite was estimated as 14.19 % (Fig.

23   4B), while no signal of Ag was detected in the control (Fig. 4A).   The elements, percentage,

24   atomic weight, and series of the biocomposites were listed in the insight table of Fig. 4.

25   Morphology and size of AgNPs in the biocomposites were examined by TEM (Fig. 5).   In both

1   of the C3Ag3 and C3Ag5 biocomposites, spherical AgNPs with the sizes of 5-30 nm in diameter

2   were observed to be well distributed throughout the cellulose matrix without agglomeration, but

3   not in C3Ag1 (Fig 5A-C).   Mostly, the size of the AgNPs was <15 nm and the mean particle size

4   of C3Ag1, C3Ag3, and C3Ag5 was approximately 14.17, 11.35, and 11.08 nm, respectively.   It

5   has been reported that polymers may act as capping agents for the stabilization of AgNPs[31].   Rai

6   *et al.* discussed that the size and shape of the nanoparticles are important factors for the surface

7   chemistry and antimicrobial property[27].   AgNPs smaller than 10 nm in diameter was reported to

8   exhibit electronic effect when they interact with bacteria, thereby enhancing the reactivity.

9   Truncated triangular nanoparticles exhibited the most effective antibacterial activity, followed by

10   spherical, and then rod shaped ones.   The size distribution of the biocomposites was shown in

11   Fig. 5D.   More uniform size of AgNPs could be obtained when higher amount of $AgNO_3$ was

12   used in SPP.

13

14   **3.3. Antibacterial activity of cellulose/AgNP biocomposites**

15   Based on the physical and chemical characterization of the biocomposites (Table 2),

16   antimicrobial assays were carried out using C3Ag1, C3Ag3, and C3Ag5.   The cellulose/AgNP

17   biocomposites were analysed for their antibacterial property against gram negative (*E. coli, P.*

18   *aeruginosa, V. parahaemolyticus*) and gram positive (*S. aureus* and *B. cereus*) pathogens, most of

19   which can cause infectious disease in human and animals via food or water poisoning.   All the

20   scaffolds of C3Ag1, C3Ag3 and C3Ag5 were subjected to agar diffusion analysis for their

21   antibacterial activity, monitoring inhibition of bacterial growth by the formation of clear zone

22   around the discs of the scaffolds (6 mm in diameter) placed on Műller-Hinton agar plates (Fig. 6A,

23   B).   C3Ag0 containing no AgNPs was used as a control.   The zone of growth inhibition caused

24   by C3Ag5 was 15 mm for *E. coli,* 14 mm for *P. aeruginosa,* 13 mm for *B. cereus,* 12 mm for *V.*

1   *parahaemolyticus* and *S. aureus*.   Generally, gram negative bacteria were inhibited more for their

2   growth than gram positive bacteria. However, in this test, the AgNPs embedded in the

3   biocomposite discs probably were not in direct contact with the cells on the plates, indicating that

4   the size of the clear zone might not be proportional to the antibacterial efficacy of the

5   biocomposites.   The antibacterial effect of AgNPs was likely to be exhibited through the particle

6   itself by turning into Ag^+ ions and generating reactive oxygen species.   They also would disturb

7   growth signaling pathway inside the bacterial cell by modulating tyrosine phosphorylation of

8   proteins that are important for cell viability[35].

9   MIC of the cellulose/AgNP biocomposites was also determined using C3Ag5.   LB broth (5

10   ml) was inoculated with 1/50 volume of overnight culture of each pathogen and various

11   concentrations of AgNPs (0–81.6 μg/ml) was added to each tube.   Then, the tubes were

12   incubated at 37°C for 24 h with gentle shaking (150 rpm) and turbidity of each tube was visually

13   observed.   The biocomposites of C3Ag5 showed MIC of 5.1 μg/ml for gram negative bacteria

14   (*E. coli, P. aeruginosa,* and *V. parahaemolyticus*), and 15.4 and 20.4 μg/ml for gram positive

15   bacteria *B. cereus* and *S. aureus*, respectively (Table 3).   Generally, gram positive bacteria are

16   considered to be more resistant to antibacterial agent than gram negative bacteria due to thicker

17   cell wall they have.   In previous study, gelatin/AgNP biocomposite (G3Ag5) showed MIC of 20

18   μg/ml for *E. coli* and 40 μg/ml for *S. aureus*[26], suggesting that the cellulose/AgNP biocomosite

19   was more effective as an antibacterial agent.

20   The kinetics of CFU reduction by the biocomposite was examined using two bacteria, *E. coli*

21   and *S. aureus*, by time course assay of the bactericidal effect for 16 h (Fig. 7).   The *E. coli* cells

22   were affected more drastically than those of *S. aureus*.   Almost all the *E. coli* cells (99.9%) were

23   killed in 2 h incubation by all types of the biocomposites tested (Fig. 7A), while CFU of *S. aureus*

24   was reduced gradually during the period of 16 h (Fig. 7B).   Complete reduction of the *E. coli* and

25   *S. aureus* cells was observed in 4 and 16 h of incubation, respectively, under the conditions of the

1   experiments (Fig. 7).   For *S. aureus*, the more the AgNPs present, the faster the reduction rate of

2   CFU was.   Silver probably has played an active role in inhibiting bacterial growth by binding

3   covalently to the cell surface and eventually disrupting the cell memebrane[36].   An attached agent

4   disrupts the cell membrane of the bacterial cells by physical and ionic phenomenon[36].   Silver

5   ions were reported to interact with the thiol group of enzymes and proteins in the membrane and

6   cytoplasm that are important for bacterial respiration and transportation of various substances

7   across the membrane.   Moreover, silver ions have been known to be effective in preventing

8   infection of wounds[37, 38]

9

10   **3.4. Antifungal activity of cellulose/AgNP biocomposites**

11   Cellulose/AgNP biocomposites were analysed for their antifungal property against two

12   pathogens; a yeast, *C. albicans* and a mold, *A. parasiticus*.   No obvious clear zone of growth

13   inhibition was observed against both *C. albicans* and *A. parasiticus* in agar diffusion analysis (Fig.

14   6C, D).   Especially, *A. parasiticus* showed immature spore formation around the biocomposite

15   discs, suggesting that AgNPs did not inhibit the growth, but affect differentiation of the fungus.

16   When the samples from the yellow or green part of the plate were examined by a light microscope,

17   much less spores were present in the yellow part than in the green part.   Therefore, the

18   biocomposites were not likely to be effective on the retardation of the eukaryotic cell growth as

19   much as they were on bacterial growth.   MIC of the biocomposites against *C. albicans* and *A.*

20   *parasiticus* was determined as 81.6 μg/ml and 255.0 μg/ml, respectively (Table 3), which was

21   much higher than those for the bacteria.   The results also suggested that the biocomposites did

22   not affect fungal growth as effectively as bacterial growth.   The results implied that the

23   biocomposites might be safe to human cells at the concentrations effective for killing bacterial

24   pathogens.

25   Effect of the biocomposite on hyphal growth of *A. parasiticus* was tested by placing a block of

1   the fungal hyphae (6 mm) on a PDA plate that had been smeared with C3Ag5 biocomposites (Fig.

2   8).   In 3 days of incubation at room temperature, hyphal growth began to be observed around the

3   fungal block.   In 7 days, fungal hypha was extended to ~39 mm in diameter with green

4   pigmentation, indicating sporulation in progress on the control plate with no biocomposite

5   smeared (Fig. 8A).   However, the growth was retarded by the biocomposites, showing growth to

6   a diameter of <11 mm and taking yellow color during the same period of culture (Fig 8B-D).

7   Previously, damage of spores by nanocomposites was reported to be associated with disruption of

8   cell wall, leading to leakage of the cytoplasmic content subsequently to cell death[39,40].   This

9   effect was more pronounced by increasing the AgNPs content in the films[39].

10

11   **4. Conclusion**

12   Cellulose/AgNP biocomposites were successfully synthesized using various concentrations of

13   cellulose and $AgNO_3$ by an eco-friendly one-step process of solution plasma.   AgNPs were

14   synthesized in the cellulose matrix by discharging plasma for a very short time of 180 s in the

15   solution.   The advantage of SPP for the generation of nanoparticles was not only its rapidity but

16   also no need for additional hazardous chemicals as a reducing or a stabilizing agent.   3D

17   scaffolds of the biocomposites were formed by a simple lyophilization process.   Analyses on the

18   micro-porous structure, elemental percentage, intensity, and purity of the nanobiocomposites

19   confirmed their physico-chemical properties that were suitable for stability and functionality as

20   reactive agent.   Spherical nanoparticles that were well distributed without agglomeration were

21   observed by TEM and they had a size range of 5-30 nm in diameter.   The size of pore and

22   nanoparticles in the biocomposites were likely to be modulated by the concentrations of cellulose,

23   the matrix, and $AgNO_3$, the precursor in the solution.   The cellulose/AgNP biocomposites

24   exhibited a broad spectrum of antimicrobial activity against various pathogens, being most

16

1   effective against gram negative bacteria, and then in the order of gram positive bacteria, *C.*

2   *albicans,* and *A. parasiticus*.   The two fungi were quite resistant to the nanobiocomposite,

3   implying that they might not be toxic to human cells.   The results suggested that the

4   cellulose/AgNP biocomposites had potential for application as a topical antibacterial agent or

5   wound dressing materials with antibiotic activity that does not induce drug resistance among

6   pathogenic bacteria.   From all the results obtained in this study, SPP seemed to be the most

7   effective and safest way to synthesize polymer based metal nanoparticle composites that can be

8   applied to biomedicine.

9

10   **Acknowledgement**

13

14   **References**

15   1. D. MubarakAli, J. Arunkumar, K. HarishNag, K.A. SheikSyedIshack, E. Baldev, D. Pandiaraj,

16   N. Thajuddin, Colloid. Surf B: Biointerfaces., 2013, **103,**   166.

17   2. M. Jeyaraj, G. Sathishkumar, G. Sivanandhan, D. MubarakAli, M. Rajesh, R. Arun, G.

18   Kapildev, M. Manickavasagam, N. Thajuddin, K. Premkumar, A. Ganapathi, Colloid. Surf B:

19   Biointerfaces., 2013, **106,** 86.

20   3. T.B. Henry, F.M. Menn, J.T. Fleming, J. Wilgus, R.N. Compton, G.S. Sayler, *Environ. Health*

21   *Perspect,* 2007, **115,**   1059.

22   4. S.C. Kim, J.W. Kim, G.J. Yoon, S.W. Nam, Curr. Appli. Phys., 2013, **13,** 548.

23   5. Y. Wei, X. Zuo, X. Li, S. Song, L. Chen, J. Shen, Y. Meng, Y. Zhao, S. Fanf, Mat. Res. Bull.,

24   2014, **53,** 145.

6. P. Pootawang, S.C. Kim, J.W. Kim, S.Y. Lee, J. Nanosci and Nanotech., 2013, **13,** 589.

7. O. Takai, Pure Appl. Chem., 2008, **80,** 2003.

8. P. Prasertsung, S. Damrongsakkul, N. Saito, Polymer Degra. Stabili., 2013, **98,** 2089.

9. X. Ma, F. Wu, J. Roth, M. Gell, E.H. Jordon, Surface. Coat.   Tech., 2006, **201,**   4447.

10. P. Pootawang, N. Saito, O. Takai, S.Y. Lee, Nanotechnology, 2012, **23,** 395602.

11. I. A. Hamarneh, P. Pedrow, A. Eskhan, N. A. Lail, Surface. Coat. Tech., 2013, **234**, 33.

12. T. Demina, D. Z. Zotova, M. Yablokov, A. Gilman, T. Akopova, E. Markvicheva, A. Zelenetskii, Surface. Coat. Tech. 2012, **207**, 508.

13. J. Julale, V. Scholtz, Clin. Plas. Med. 2013, **1**, 31.

14. E. Omurzak, J. Jasnakunov, N. Mairykova, A. Abdykerimova, A. Maatkasymova, S. Sulaimankulova, M. Matsuda, M. Nishida, H. Ihara, T. Mashimo, J Nanosci Nanotechnol., 2007, **7**, 3157.

15. S.M. Kim, G.S. Kim, S.Y. Lee, Mater. Lett., 2008, **62**, 4354.

16. P. Pootawang, N. Saito, S.Y. Lee, Nanotechnology, 2013, **24,** 055604.

17. J.H. Kim, S. Yun, H.U. Ko, J. Kim, Curr. App. Phy., 2013, **13,** 897.

18. S. H. Jin, S.M. Kim, S. Y. Lee, J.W. Kim, J. Nanosci and Nanotech, 2014, **14**, 8094.

19. P. Pootawang, Y.S, Lee, Mater. Lett., 2012, **80,** 1.

20. P. Pootawang, N. Saito, O. Takai, S.Y. Lee, Mat Res. Bull., 2012, **47**, 2726.

21. P. Pootawang, N. Saito, O. Takai, Y.S. Lee, Nanotechnology, 2012, **23,** 395602.

22. L. Chen, T. Mashimo, H. Okudera, C. Iwamoto, E. Omurzak, *RSC Adv,* 2014, **4,** 28679.

23. L. Chen, T. Mashimo, E. Omurzak, H. Okudera, C. Iwamoto, A. Yoshiasa*, J. Phys. Chem. C.,* 2011, **115,** 9370.

24. Z. Kelgenbaeva, E. Omurzak, S. Takebe, Z. Abdullaeva, S. Sulaimankulova, C. Iwamoto, T. Mashimo, *Jpn. J. Appl. Phys.,* 2013, **52,** 11NJ02. doi:10.7567/JJAP.52.11NJ02.

25. B.H. Lee, H.J. Kim, H.S. Yang, Curr. App. Phy., 2012, **12,** 75.

1 26. S.C. Kim, S.M. Kim, G.J. Yoon, S.W. Nam, S.Y. Lee, J.W. Kim, Curr. Appli. Phys., 2014, **14**,

2   S172.

3 27. M. Rai, A. Yadav, A. Gade. Biotech. Adv., 2009, **27,** 76.

4 28. P. Pootawang, N. Saito, O. Takai, Mater. Lett., 2011, **65**, 1037.

5 29. McFarlands, J., J. Amer. Med. Assoc. 1907, **14**, 1176.

6 30. C. Chinkap, L. Myunghee, K.C. Eun, Carbohydr Polym., 2004, **58**,   417.

7 31. D. MubrakAli, J. Arunkumar, M. Rahuman Sheriff, D. Pandiaraj, K.A. ShiekSyedIshack, N.

8   Thajuddin, Pharma Nanotech., 2013, **1**, 78.

9 32. S.M. Oliveira, R.L. Reis, J.F. Mano, ACS Biometer. Sci. Eng. 2015, **1**, 2

10 33. C. J. Grande, F.G. Torres, C.M. Gomez, M. Carmen Bano, *Acta Biomater*. 2009, **5**, 1605.

11 34. K. Nakagawa, M. Iwamoto, A. Nakajima, K. Shono, K.J. Satoh, Colloid Interface Sci., 2004,

12   **278,** 198.

13 35. S. Shrivastava, T. Bera, A. Roy, G. Singh, P. Ramachandrarao, D. Dash, Nanotech, 2007, **18**,

14   225103

15 36. S. Sarkar, A.D. Jana, S.K. Samnata, G. Mostafa, Polyhedron, 2007, **26**, 4419.

16 37. S.L. Percival, P.G. Bowler, D. Russel, J. Hospi. Infec., 2005, **60**, 1.

17 38. J.B.Wright, K. Lam, D. Habsen, R.E. Burrell, Ameri. J. Infec. Cont., 1999, **24,** 344.

18 39. V. Gopinath, P. Velusamy, Spectrochima Acta A., 2013, **106**, 170.

19 40. D. MubarakAli, N. Thajuddin, K. Jeganathan, M. Gunasekaran, Colloid. Surf B:
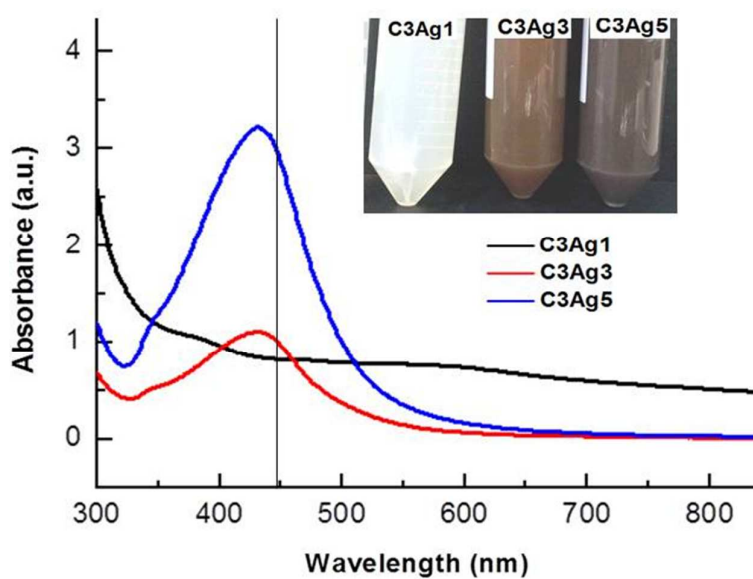
20   Biointerfaces., 2011, **85,**   360.

Fig. 1 UV-Vis spectra of the cellulose/AgNP biocomposites: The nanobiocomposites, C3Ag1, C3Ag3, C3Ag5 had surface plasmon resonance at 350-450 nm. Insight picture showed the biocomposites turned to brown color based on the AgNPs concentration in the solution by plasma discharge.
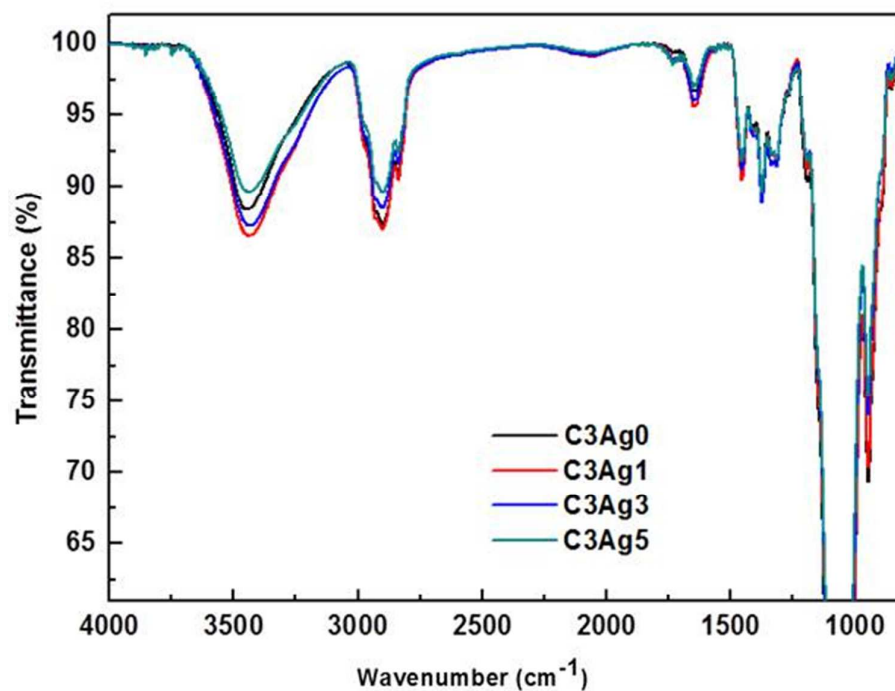
Fig. 2 FTIR spectra of the cellulose/AgNP biocomposites: Characteristic vibration (1409 cm^{-1} and 1053cm^{-1}) of cellulose was used as a control (C3Ag0).   C-H bending and C-OH bending were due to the interaction of functional groups with AgNPs in the nanobiocomposites of C3Ag1, C3Ag3, and C3Ag5.
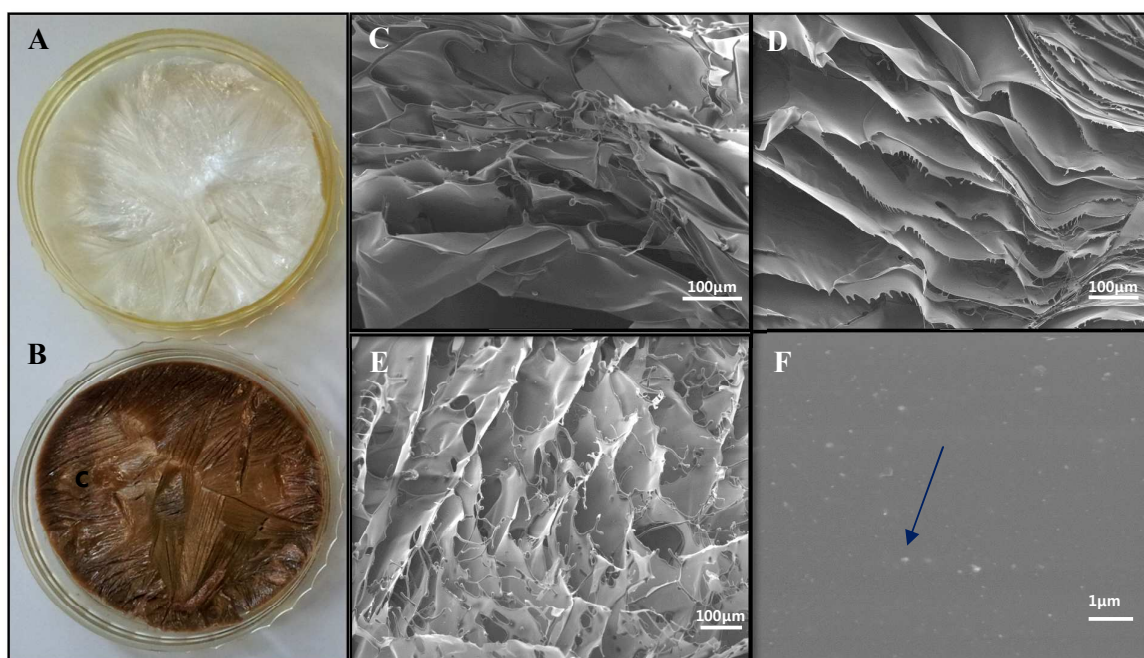
Fig. 3   Structure of the 3D scaffold type biocomposite: 3D scaffolds of the control (A) and the C3Ag5 biocomposite (B) are compared. FESEM analysis showed that the micro-porous structure of C3Ag1(C) had inter-connected cross walls with blend ends; C3Ag3 (D) and C3Ag5 (E) inter-connected cross walls with micro-fibril edges. Spherical AgNPs was observed encrusted on the matrix of C3Ag5 (F).   Size of the micro-pore was dependent on the concentration of silver.
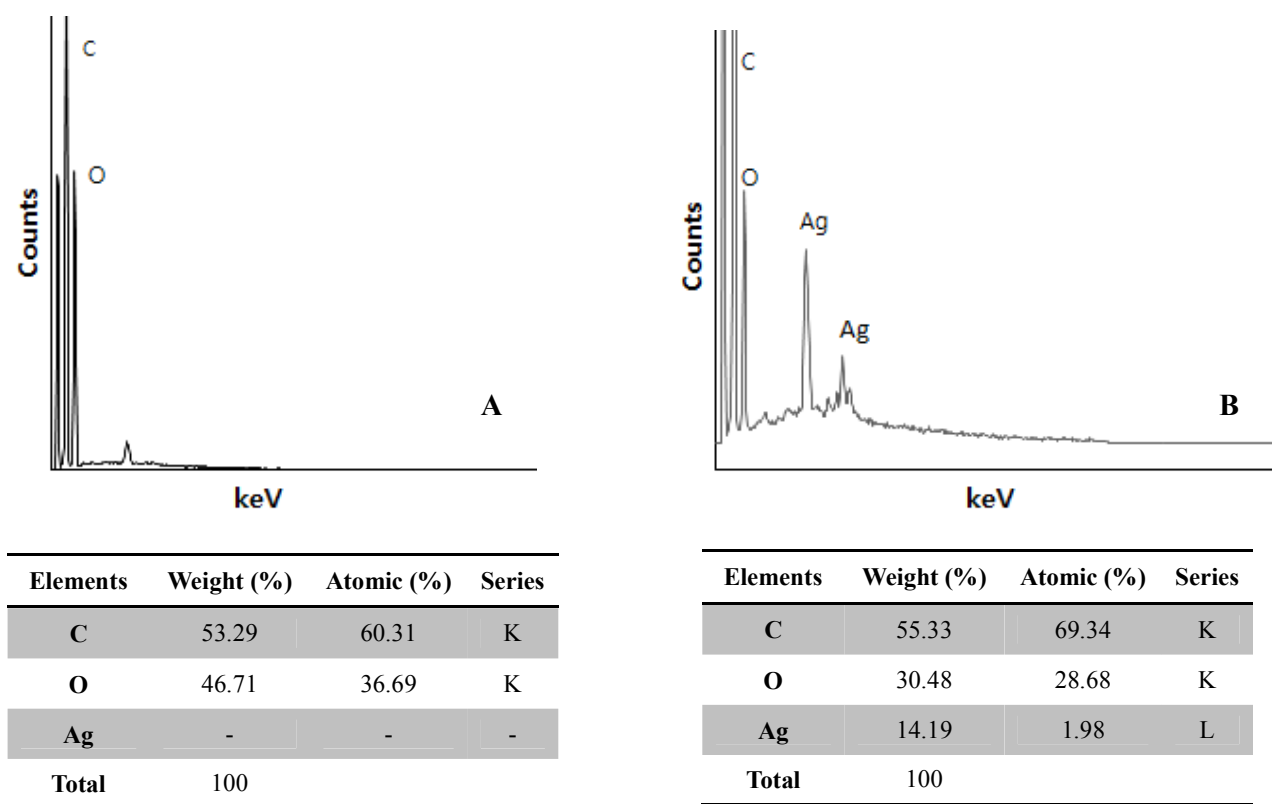
Elements	Weight (%)	Atomic (%)	Series
C	53.29	60.31	K
O	46.71	36.69	K
Ag	-	-	-
Total	100		

Elements	Weight (%)	Atomic (%)	Series
C	55.33	69.34	K
O	30.48	28.68	K
Ag	14.19	1.98	L
Total	100		

Fig. 4 EDS analysis of the C3Ag5 biocomposites: Elemental signal and percentage of cellulose without AgNPs (A) and cellulose/AgNP biocomposite (B).
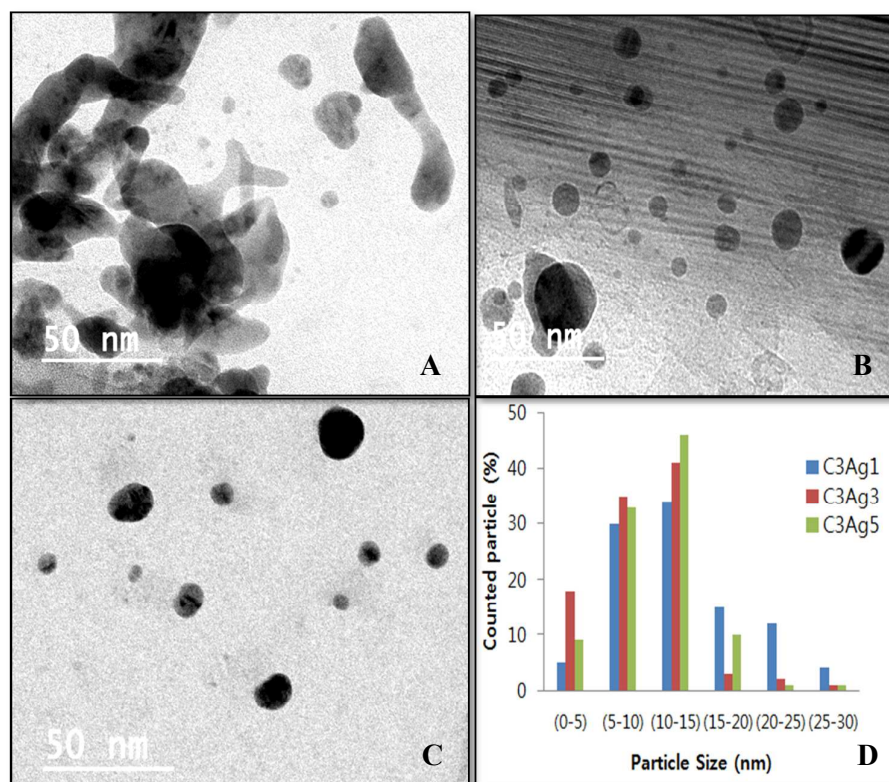
Fig. 5   TEM analysis of AgNPs in the biocomposites: The size and shape of AgNPs in the biocomposites were observed after removal of cellulose.   The C3Ag1 biocomposite had agglomerated particles with average size of 14.17 nm (A); C3Ag3, anisotropic spherical particles of 11.35 nm (B); and C3Ag5, stable spherical particles of 11.08 nm (C).   The graph represents size distribution of the particles in the 3 nanobiocomposites (D).
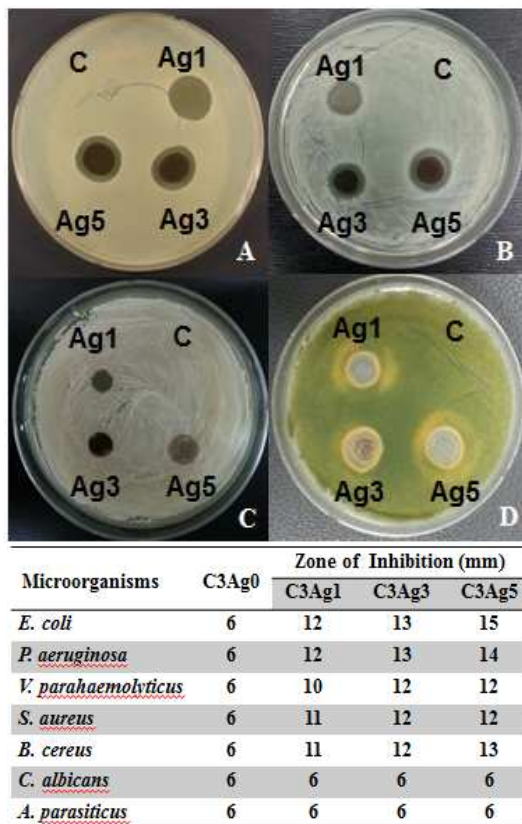
Microorganisms	C3Ag0	Zone of Inhibition (mm)		
		C3Ag1	C3Ag3	C3Ag5
E. coli	6	12	13	15
P. aeruginosa	6	12	13	14
V. parahaemolyticus	6	10	12	12
S. aureus	6	11	12	12
B. cereus	6	11	12	13
C. albicans	6	6	6	6
A. parasiticus	6	6	6	6

Fig. 6 Zone of growth inhibition formed by the cellulose/AgNP discs: Various degrees of anti-biogram pattern were observed by the C3Ag1, C3Ag3 and C3Ag5 discs against various pathogenic microorganisms, *E. coli* (A), *S. aureus* (B), *C. albicans* (C), *A. parasiticus* (D). Insight table compares the sizes of the zone of inhibition formed by discs against various pathogens.
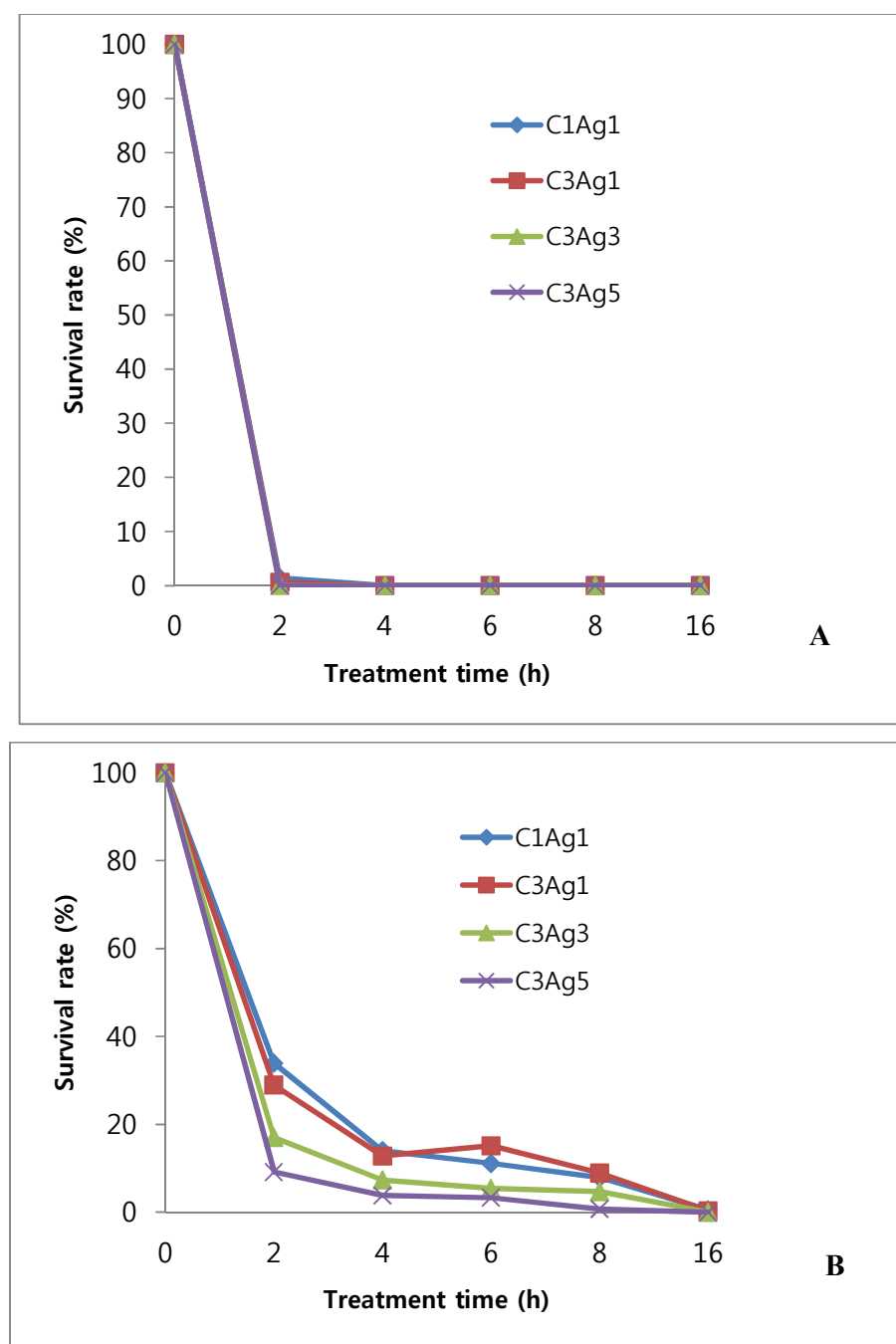
Fig. 7   Bactericidal effect of cellulose/AgNP biocomposites: Reduction of CFU by the C3Ag5 biocomposite was examined against *E. coli* (A) and *S. aureus* (B). Both bacteria were cultured at 37°C by adding 5.1 μg/ml (*E. coli*) and 20.4 μg/ml (*S. aureus*) of AgNPs.
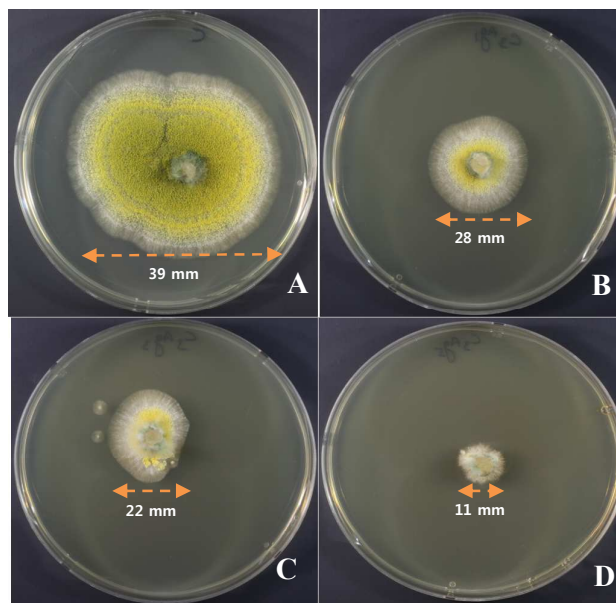
Fig. 8   Effect of cellulose/AgNPs biocomposites on hypal growth of *A.parasiticus*: On the center of a PDA plate smeared with no biocompoiste (A), C3Ag1 (B), C3Ag3 (C), or C3Ag5 (D), a small block of the fungal hyphae (6 mm in diameter) was placed and incubated for 3 days at 25°C.

Table 1 Summary of the synthesis of nanomaterials (metals, oxides, composites, polymers) and their size and application using plasma in liquids**.**

Nanomaterials synthesized	Size of the materials	Applications	References
Metal nanoparticles:			
C60	7 nm	Conductivity	29
Au	15 nm	Catalytic property	30
Cu	33.7 ± 5.8 nm	Material engineering	17
Ni	10-200 nm	Semi-herogenous catalysis	31
Ag	61.8 ± 21.8 nm	Sensors	32
Metal-Metal nanocomposites			
Ag/Pt	5 nm	Heterogenous catalytic activity	33
Ag/Si	20 nm	Catalytic property	34
Pt/C	38.14 nm	Membrane fuel cells	35
Metal oxide nanoparticles			
WO_3	5 nm	Solar energy	36
ZrO_2	5 nm	Solar energy	37
Fe_3O_4	19 nm	Magnetic and optics	38
Polymer-Polymer nanocomposites			
Cellulose/aniline	100-200 nm	Electrical conductivity	39
Polymer-Metal nanocomposites			
Gelatin/Ag	10-15 nm	Antimicrobial	4, 14
Cellulose/Ag	5-20 nm	Broad spectrum of antimicrobial property	This study

Table 2. Comparison of the properties of nanobiocomposites synthesized using various
concentrations of cellulose and silver.

Nanobiocomposites	Scaffold formation	Antimicrobial property	Nanoparticles formed
Cellulose (1%)			
1 mM, 3 mM, 5 mM	Fragile	Poor	Agglomeration
Cellulose (2%)			
1 mM, 3 mM, 5 mM	Fragile	Intermediate	No agglomeration
Cellulose (3%)			
1 mM, 3 mM, 5 mM	Stable and firm	Excellent	No agglomeration

Table 3. MIC of cellulose/AgNP biocomposites

Microorganisms	MIC : C3Ag5 AgNPs (µg/ml)
E. coli	5.1
P. aeruginosa	5.1
V. parahaemolyticus	5.1
S. aureus	20.4
B. cereus	15.3
C. albicans	81.6
A. parasiticus	255.0